Adhesive Dynamics Simulation of Neutrophil Arrest with Deterministic Activation

Ellen F. Krasik, Ka Lai Yee, and Daniel A. Hammer
Department of Bioengineering, University of Pennsylvania, Philadelphia, Pennsylvania

ABSTRACT The transition from rolling to firm adhesion is a key element of neutrophil activation and essential to the inflammatory response. Although the molecular mediators of rolling and firm adhesion are known to be selectins and β_2-integrins, respectively, the precise dynamic mechanism by which these ligands facilitate neutrophil arrest remains unknown. Recently, it has been shown that ligation of E-selectin can stimulate the firm adhesion of neutrophils via a MAP-kinase cascade. To study the possible mechanism by which neutrophil arrest could occur, we created an integrated model by combining two methodologies from computational biology: a mechanics-based modeling of leukocyte adhesion (adhesive dynamics) and signal transduction pathway modeling. Within adhesive dynamics, a computational method our group has shown to accurately recreate rolling dynamics, we include a generic, tunable integrin activation module that links selectin engagement to integrin and activity. This model allows us to relate properties of the activation function to the dynamics of rolling and the time and distance rolled before arrest. This integrated model allows us to understand how intracellular signaling activity can set the timescale of neutrophil activation, adhesion, and diapedesis.

INTRODUCTION

For a neutrophil to perform its phagocytic function in the tissue, it must exit the bloodstream. In response to inflammatory chemokines, endothelial cells in venules upregulate and present E- and P-selectin on their luminal surfaces. Leukocytes expressing the selectins' glycosylated ligands transit though the vasculature and interact with the endothelium through transient receptor-ligand bonding, a behavior otherwise known as rolling. Selectin-mediated rolling is followed by integrin-mediated firm adhesion and subsequent leukocyte extravasation and chemotaxis to the site of tissue injury.

The transition from rolling to firm adhesion results from β_2-integrin activation, during which a conformational change in the integrin improves its affinity for intercellular adhesion molecule-1 (ICAM-1), its endothelial ligand. The structure of the resting integrin resembles a folded switchblade, such that upon activation, the α and β cytoplasmic domains separate, and the protein swings open into an extended conformation, freeing the N-terminal headpiece from the C-terminal, membrane-proximal domain (1,2). Studies of rolling in cells transfected with wild-type, locked-open (extended), and locked-closed conformations of leukocyte function-associated antigen-1 (LFA-1) showed that the conformational presentation of I-domain, the ICAM-binding region in the integrin headpiece, indeed regulates the transition from rolling to firm adhesion (3). When I-domain was sequestered in the locked-closed or wild-type conformations, it mediated rolling adhesion; the locked-open conformation supported firm adhesion. Recent work suggests that rolling and firm adhesion mediated by LFA-1 result from two separate extended conformations that differ in the I-domain affinity for ICAM-1 (4).

The two major activation hypotheses both suggest that an input signal, accumulated from the rolling neutrophil's surface receptors' sampling of the endothelial surface, must be processed by the cell to make the important decision: to stop or not to stop (5,6). The first hypothesis suggests that ligation of selectins activates a signaling pathway that causes the global activation of β_2-integrins, which results from a conformational change yielding increased binding affinity. The second posits that interactions between endothelium-presented chemokines and specific leukocyte G-protein coupled receptors (GPCRs) release integrins from cytoskeletal restraints, thus promoting mobility and clustering, thereby locally enhancing integrin avidity. Immobilized interleukin 8 (IL-8) was shown to activate neutrophils rolling on surfaces coated with immobilized P-selectin and ICAM-1 (7). In addition, stimulation of neutrophils with IL-8 and allosteric induction of the activated conformation of LFA-1 demonstrated that the topography and lifetime of high-affinity LFA-1 regulated neutrophil capture efficiency (i.e., transition to firm adhesion) (8). In vivo observations of rolling neutrophils in CXCR2 and E-selectin knockout mice suggest that the chemokine- and E-selectin-mediated arrest mechanisms overlap (9).

Recent experimental evidence points to the p38 mitogen-activated protein kinase (MAPK) cascade as a signaling pathway involved in global integrin activation mediated by P-selectin glycoprotein ligand-1 (PSGL-1), L-selectin, and the E-selectin ligand. When bound by mAb blocking the P-selectin binding site, PSGL-1 was shown to transmit a

Submitted July 20, 2005, and accepted for publication March 3, 2006.

Address reprint requests to Daniel A. Hammer, Dept. of Bioengineering, University of Pennsylvania, 120 Hayden Hall, 3320 Smith Walk, Philadelphia, PA 19104. Tel.: 215-573-6761; Fax: 215-573-2071; E-mail: hammer@seas.upenn.edu.

0006-3495/06/08/1145/11 $2.00

doi: 10.1529/biophysj.105.070706

signal into leukocytes via a MAPK cascade; when bound by P-selectin, it enhanced tyrosine phosphorylation (10). Ligation of PSGL-1 by P-selectin was also shown to activate Mac-1 (11), and ligation of P-selectin on murine neutrophils enhanced integrin-mediated adhesion (12). A p38 MAPK inhibitor blocked L-selectin-activated Mac-1-dependent adhesion (13). Simon and co-workers (14) demonstrated that cell arrest on surfaces expressing both E-selectin and ICAM-1 is dependent on E-selectin-mediated rolling, activation of the p38 MAPK cascade, and activation of LFA-1 and Mac-1. These investigators next determined that p38 MAPK-dependent adhesion increased with the application of shear stress, thus demonstrating a link between hydrodynamic forces and signaling of neutrophil adhesion (15).

The MAPK cascade, a well-conserved signaling pathway, is involved in a wide variety of cell responses, such as proliferation, apoptosis, and migration (16). Mathematical modeling of the basic MAPK cascade demonstrates switch-like cooperative kinetics, a property well-suited for decision-making (17). Without assuming cooperative regulation of individual enzymes, the model predicts for the cascade an overall stimulus-response curve with a Hill coefficient as high as 5 (17), a strong dependence referred to as ''ultrasensitivity''.

For simplicity, we choose to model the MAPK cascade as a modular Hill function that couples E-selectin ligation with β_2-integrin activation. For our model of neutrophil activation, selectin ligation during rolling is the input signal; integrin activation and subsequent adhesive state are the output response. The function modularity will allow us to specify freely the input-output relationship, with control over its timescale, degree of cooperativity, and dependence on bond formation. In effect, this model casts the endothelium as the master regulator of activation: by regulating its surface expression of selectin, it increases the number of selectin bonds (the cascade input) and enhances the rate of integrin activation. By permitting a generic yet tunable activation function, we will be able to approximate experimental data more simply and to incorporate more easily future information regarding details of the activation pathway.

Two different β_2-integrins on the neutrophil, LFA-1 (CD11a/CD18) and Mac-1 (CD11b/CD18), mediate the firm adhesion required for extravasation. They initially exist in a resting, low-affinity state; upon activation, they shift to a high-affinity state, thus facilitating deceleration and arrest. In addition, the surface expression of Mac-1, but not of LFA-1, may rapidly increase in response to chemokine stimulation (18,19). However, the role of LFA-1 in firm adhesion under shear stress is short-lived; maintenance of ICAM-1-mediated firm adhesion over several minutes requires Mac-1 (19,20). Although these two different integrins are regulated in different ways, we will model them with one generic integrin. Our simulation can be extended easily in the future to account for the subtle differences in integrin behavior.

Previous adhesive dynamics (AD) simulations described the behavior of a neutrophil with two receptor-ligand pairs (i.e., selectin-PSGL-1 and β_2-integrin-ICAM-1) in shear flow (21). The state diagrams produced by these simulations map the boundary between firm and rolling adhesion as a function of selectin density, ICAM-1 (or integrin) density, intrinsic reaction rates, shear rates, and reactive compliances. These steady-state adhesion state diagrams showed that the receptor-ligand pairs work synergistically to promote adhesion (21). In other words, a cell with only one receptor type, either ICAM-1 or selectin, will roll for some range of surface densities beyond which the cell achieves firm adhesion. If the second type of receptor is added to the original cell, the range of first-receptor surface densities that mediate rolling is reduced, and the cell achieves firm adhesion at a lower surface density of the initial receptor type. The specific synergism depends upon flow shear rate and integrin properties. Thus, for a given cell in one state, we can predict the change in system properties required for the transition to the other state; what remains to be determined is how that transition is effected.

Our goal in this article is to develop a novel model in which we simulate the stopping of a neutrophil. Although a wide spectrum of stimulatory inputs might influence neutrophil stopping, we will simply assume that selectin ligation can lead to integrin activation through MAPK. All integrins are lumped together into a single class that can switch from a passive to an active form. The signal cascade will be modeled as a deterministic, ultrasensitive global activation within the context of adhesive dynamics, a stochastic simulation of the mechanics of cell rolling and adhesion. We simulate the dynamics of cell pausing and adhesion as a function of signal dynamics, selectin density, and hydrodynamics. This model, in which signaling and mechanics are integrated, represents a novel paradigm for understanding how signal transduction can control mechanically driven cell behavior. Although we will focus our modeling on a global selectin-mediated pathway, note that the global and localized activation processes are not mutually exclusive and can be modeled simultaneously.

METHODS

AD (22,23) was modified to account for three receptor-ligand pairs: PSGL-1/E-selectin, resting LFA-1/ICAM-1, and active LFA-1/ICAM-1. A detailed description of the two-receptor simulation appears elsewhere (21). A model schematic appears in Fig. 1, and a brief description of the algorithm follows.

Rigid microvilli are randomly distributed on the rigid, spherical cell surface, and adhesion molecules are placed at their tips according to a Poisson distribution. At each time step, a contact zone between the cell and flat endothelium is defined, spanning many microvilli, and receptor-ligand pairs within that zone are tested for formation. All preexisting bonds are then tested for breakage. Bonds are modeled as Hookean springs, and the probabilities of breakage and formation are calculated from bond-length-dependent kinetic rates. The reverse reaction rate, k_r, takes the form of the Bell model (24):

$$k_r = k_r^0 \exp(\gamma \sigma |y - \lambda| / \kappa_B T), \quad (1)$$

where k_r^0 is an intrinsic reverse reaction rate, γ is the reactive compliance, a parameter with units of length describing the bond's sensitivity to force, σ is

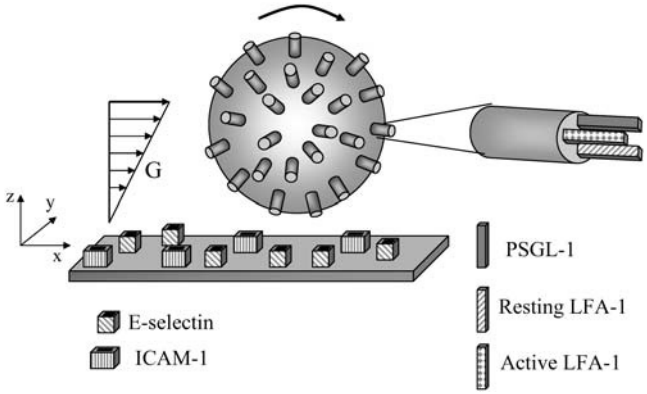

FIGURE 1 Schematic diagram of adhesive dynamics. Rigid, cylindrical microvilli are randomly placed on the surface of a sphere. Adhesion molecules are assigned randomly to these microvilli according to a Poisson distribution, and the wall is assumed to be a uniformly reactive planar surface. Length-dependent binding probabilities govern the formation and breakage of bonds. Resting integrins are activated according to a deterministic Hill function. G, shear rate.

the bond spring constant, y is the bond length, λ is the unstressed bond length, and $\kappa_B T$ is the thermal energy.

The forward reaction rate, k_f, follows from the Boltzmann distribution for affinity and takes the form of

$$k_f = k_f^0 \exp\left[\sigma\left|y - \lambda\left(\gamma - \frac{1}{2}|y-\lambda|\right)\right| \Big/ \kappa_B T\right], \qquad (2)$$

where k_f^0 is the intrinsic forward reaction rate and the remaining symbols are the same as in Eq. 1. The forward rate is further modified to incorporate the effect of relative velocity between cell and surface. Chang and Hammer (25) determined that binding rate is a function of the Peclet number (Pe = (cell radius)(relative velocity)/(lateral diffusivity)). For the conditions of this system, the binding rate is a linear function of the relative velocity. The probability of bond formation, P_f, and breakage, P_r, become $P_f = 1 - \exp(-k_f \Delta t)$ and $P_r = 1 - \exp(-k_r \Delta t)$, respectively. A short-range nonspecific repulsive force between cell and surface, gravitational force, and a surface roughness term are also included (26).

Total forces and torques exerted on the cell due to bonds, hydrodynamic flow, steric repulsion, and gravity are calculated. The equations of low-Reynolds number motion for a sphere in close contact with a wall have been solved (27,28). For hydrodynamic calculations, we employ a hydrodynamic radius equal to the sum of the cell radius and microvillus length. The rotational and translational velocities in each coordinate direction can be calculated from the component forces and torques. The positions of the cell and cell-surface receptors are then updated.

MAPK activity has been shown to follow an ultrasensitive activation with a large Hill coefficient (17). At the end of each time step, the number of PSGL-1-E-selectin bonds, S, serves as an input to the modular activation function, a Hill function:

$$\frac{dI^*}{dt} = K_{act} I \frac{S^{n_{Hill}}}{S^{n_{Hill}} + K_m^{n_{Hill}}}. \qquad (3)$$

Here, the change in mean number of active integrins per microvillus, I^*, is a function of the mean number of resting integrins per microvillus, I. The Hill function parameters are K_{act}, the activation constant, K_m, the number of selectin bonds required for half-maximal response, and n_{Hill}, the Hill coefficient, or measure of cooperativity. The overall activated fraction of integrins is calculated from the updated mean numbers of molecules per microvillus. To determine the number of integrins on an individual microvillus that should be active, the total number of integrins on that microvillus is multiplied by the overall activated fraction and rounded to the nearest whole number. We assume that bound resting integrins activate just like free integrins, so the number of bound and free activated integrins reflects the microvillus-specific fractions of bound and free molecules. Resting and activated integrins will have different mechanochemical properties, which will lead to changes in adhesiveness as the integrins become activated.

Parameters

Table 1 lists system parameters used in these simulations. The cell radius is that of a neutrophil. Microvillus density and length are chosen to match experimental measurements (29). The shear rate of 100 s^{-1} falls within the range of shear rates at which neutrophil rolling is observed (30) but below the values where significant cell deformation occurs (31).

Molecular binding parameters are shown in Table 2. The Bell model parameters, γ and k_r^0, for the E-selectin-PSGL-1 and ICAM-1-resting LFA-1 pairs are taken from pause-time distribution analysis and atomic force microscopy measusrements, respectively (32,33). The value of k_r^0 for ICAM-1-active LFA-1 is also taken from Zhang and co-workers (33). To determine two-dimensional k_f^0 values for the selectin and resting integrin binding pairs, simulations employing the measured Bell model parameters were fit to data from experiments of cell-free rolling mediated by molecular pairs E-selectin and PSGL-1 or ICAM-1 and wild-type LFA-1 I domain (34,35). Measurements of ICAM-1 binding to resting and active LFA-1 in solution indicate that there is a 9000-fold increase in affinity for ligand from the resting to active integrin state (36,37). Using this information along with the previously determined rate constants, we then calculate a k_f^0 value of 115 $\mu m^2/s$ for the ICAM-1-active LFA-1 bond. LFA-1 in the passive state can support rolling interactions in ICAM-1, consistent with what has been observed experimentally (35,36). The densities of PSGL-1 and LFA-1 on the tips of microvilli are based on measurements of PSGL-1 density or the random distribution of LFA-1 across the entire cell. LFA-1 molecules not on microvilli tips are irrelevant since they are too far from the ligand surface for binding on the timescale of the most simulations (21,36,45).

RESULTS

State diagram

Before investigating the role of deterministic activation in neutrophil arrest, we first must establish the adhesive behaviors of both a fully resting system, where all integrins are resting, and a fully activated system, in which all integrins are active. We calculate an adhesion state diagram as a

TABLE 1 Simulation parameters

Parameter	Definition	Value	References
a	Cell radius	5 μm	(43)
G	Shear rate	100 s^{-1}	(26,30)
μ	Viscosity	1 cP	–
ρ	Fluid density	1.0 g/cm^3	–
$\Delta\rho$	Density difference	0.05 g/cm^3	–
ε_w	Wall roughness'	50 nm	(26)
σ	Spring constant	100 dyne/cm	(44)
λ	Equilibrium bond length	70 nm	(45)
T	Temperature	298 K	–
ρ_{MV}	Microvillus density	5 MV/μm^2	(29)
L_{MV}	Microvillus length	0.3 μm	(29)
$n_{E\text{-}sel}$	E-selectin surface density	3600 molecules/μm^2	(34)
n_{ICAM}	ICAM-1 surface density	210 molecules/μm^2	(35)

TABLE 2 Molecular binding parameters

Molecule pair	γ (Å)	k_r^0 (s^{-1})	k_f^0 ($\mu m^2/s$)
E-selectin::PSGL-1	0.18*	2.6*	0.06†
ICAM-1::resting LFA-1	0.1†	4.0‡	0.3†
ICAM-1::active LFA-1	2.1‡	0.17‡	115§

*From pause time distribution analysis (32).
†From AD fitting to cell-free rolling data (34,35).
‡From atomic force microscopy measurements (33).
§Calculated from measured increase in affinity (36,37).

function of selectin and integrin density for both fully resting and fully active states (Fig. 2). As noted in Methods, fractional numbers of molecules per microvilli mean that the actual number for each microvillus (MV) is sampled from a Poisson distribution and rounded to the nearest whole number. A 10-s mean rolling velocity that is 2% of the hydrodynamic velocity, V_H, parameterizes the boundaries separating the states of rolling and firm adhesion. The dashed curve represents the arrest boundary for resting LFA-1, and the solid curve represents the boundary for active LFA-1. Both boundaries demonstrate the synergistic function of selectins and integrins in securing adhesion, as pointed out in previous AD work (21). The shift of the solid curve (active integrins) to the left of the dotted line (inactive integrins) indicates fewer integrins are needed for firm arrest if the integrins are active. This diagram permits the selection of appropriate cell receptor densities that can lead to either a rolling or firmly adherent state, depending upon the integrin activation state. In this diagram, we choose a PSGL-1 density of 1 molecule/MV and a total LFA-1 density of 2 molecules/MV (*solid triangle*). When all integrins are resting in this combination, the cell rolls at 43 ± 6 μm/s with a mean number of selectin bonds $\bar{S} = 1.7 \pm 0.3 (N = 10)$. When all integrins are active, the cell is firmly adherent (velocity $< 0.02 V_H$).

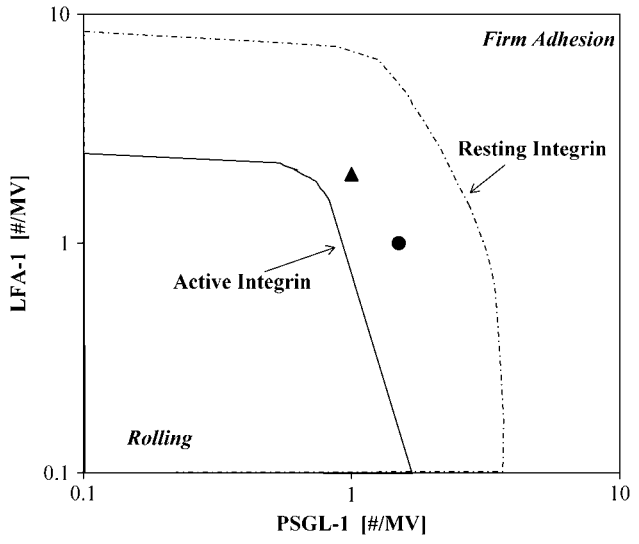

FIGURE 2 State diagram depicting the boundary between rolling and firm adhesion as a function of PSGL-1 and LFA-1 site densities for both resting (*dashed curve*) and active (*solid curve*) integrin states. For each integrin state, the boundary represents a 10-s mean velocity of $0.02 V_H$. The point indicated by the triangle corresponds to a cell with receptor densities of 1 PSGL-1 molecule/MV and 2 total LFA-1 molecules/MV.

Representative simulation output

Trajectories of two representative rolling and arresting neutrophils are shown in Fig. 3. For all simulations, data is recorded every 0.1 s. We define arrest as the point at which the 2-s moving average velocity falls below $0.02 V_H$. In the ''no activation'' simulations, the neutrophil has a PSGL-1 density of 1 molecule/MV and total LFA-1 density of 2 molecules/MV, all in the resting state, and the LFA-1 is not permitted to activate. These neutrophils continuously roll, and the distance traveled increases with time. The arresting neutrophil begins with identical adhesion-molecule surface densities, but a deterministic activation function ($n_{Hill} = 3$, $K_m = 3$, $K_{act} = 0.05\ s^{-1}$) is included, driving the integrins from the resting to the active state. In these simulations, the neutrophil rolls over the surface until sufficient integrin activation occurs, and the cell stops (Fig. 3).

Underlying the change in distance with time are changes in the receptor state and bonding with time, as illustrated in Fig. 4. Corresponding to the case where integrin bonds can be activated, the number of E-selectin and resting and active integrin bonds are followed in Fig. 4, *A–C*. Formation of all bond types increases as the cell decelerates, but there is a noticeable lag-time in the appearance of activated integrin bonds, an expected result. The activated fraction of integrins and 2-s moving average velocity are shown in Fig. 4, *D* and *E*, respectively. Note that the fraction of activated integrin

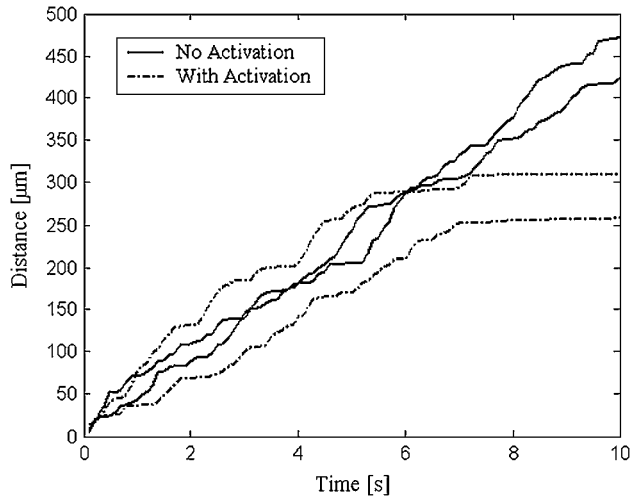

FIGURE 3 Representative dimensional simulated trajectories. Solid lines depict the case of no activation and broken lines depict the activating case ($n_{Hill} = 3$; $K_m = 3$; $K_{act} = 0.05\ s^{-1}$). PSGL-1 = 1 molecule/MV; total LFA-1 = 2 molecules/MV.

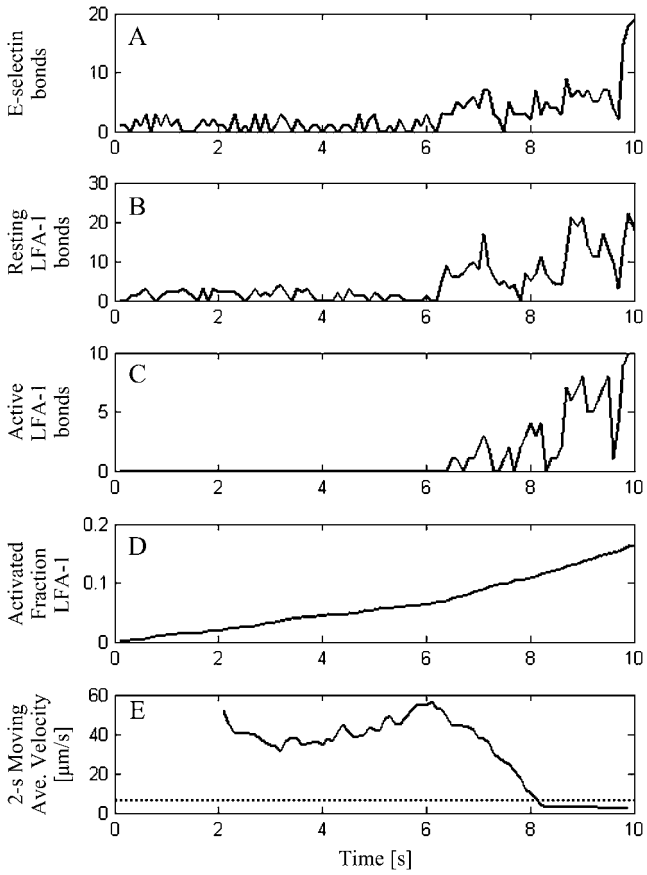

FIGURE 4 Bond formation increases and rolling velocity decreases with increasing activation. Number of selectin (*A*), resting integrin (*B*), and active integrin (*C*) bonds as a function of time. Global activated integrin fraction (*D*) and 2-s moving average velocity (*E*). PSGL-1 = 1 molecule/MV; total LFA-1 = 2 molecules/MV; $n_{\text{Hill}} = 3$; $K_{\text{m}} = 3$; and $K_{\text{act}} = 0.05$ s.$^{-1}$

does not increase as a simple exponential function asymptotically to unity. This is due to the stochastic nature of the input to the activation function: the number of selectin bonds fluctuates with time.

K_{act} determines timescale of activation and arrest

The effect of decreasing K_{act} on activation is shown for characteristic simulations in Fig. 5. With all other activation parameters held constant ($K_{\text{m}} = 3$; $n_{\text{Hill}} = 1$; PSGL-1 = 1 molecule/MV; LFA-1 = 2 molecules/MV), decreasing K_{act} fivefold (0.05 to 0.01 s^{-1}) prolongs rolling from 8 to 30.2 s (a 3.8-fold increase), whereas a 10-fold decrease (0.05 to 0.005 s^{-1}) prolongs rolling to 64.1 s (an eightfold increase). Experimental measurement of neutrophil activation determined an average rolling time before arrest of 86 s (38). Further reducing K_{act} to 0.0035 s^{-1} extended rolling time before arrest to ~91 s (Fig. 5). Thus, the value of K_{act} can be tuned to approximate the timescale of physiological behavior.

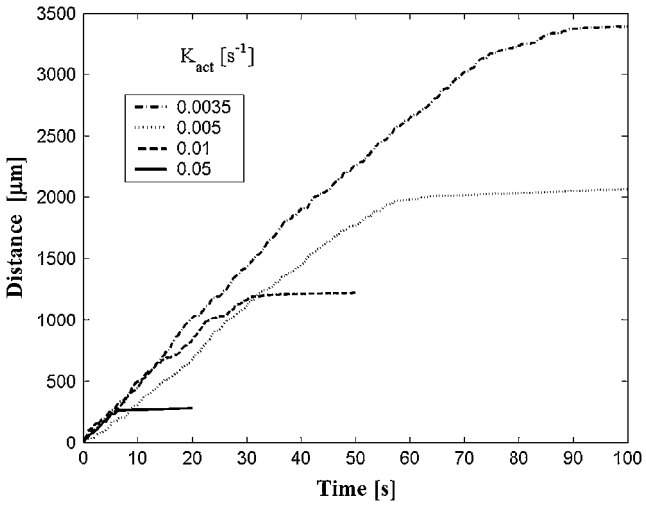

FIGURE 5 The timescale of arrest depends on K_{act}: 0.05 s^{-1} (*solid line*), 0.01 s^{-1} (*dashed line*), 0.005 s^{-1} (*dotted line*), and 0.0035 s^{-1} (*dash-dotted line*). PSGL-1 = 1 molecule/MV; total LFA-1 = 2 molecules/MV; shear rate = 100 s^{-1}; $K_{\text{m}} = 3$; $n_{\text{Hill}} = 1$.

K_{m} regulates time to arrest

The ability to tune a β_2-integrin activation function is necessary in simulating neutrophil arrest, for the physiological neutrophil is exquisitely designed to respond specifically to a distinct endothelial state. The Hill function parameter K_{m}, the number of selectin bonds required for a half-maximal integrin stimulatory response, establishes the level of E-selectin expression required to generate bonds (signals) sufficient to effect integrin activation. Fig. 6 depicts the effect of K_{m} on neutrophil trajectory at constant cell surface and endothelial receptor densities ($n_{\text{Hill}} = 3$; $K_{\text{act}} = 0.05$ s^{-1};

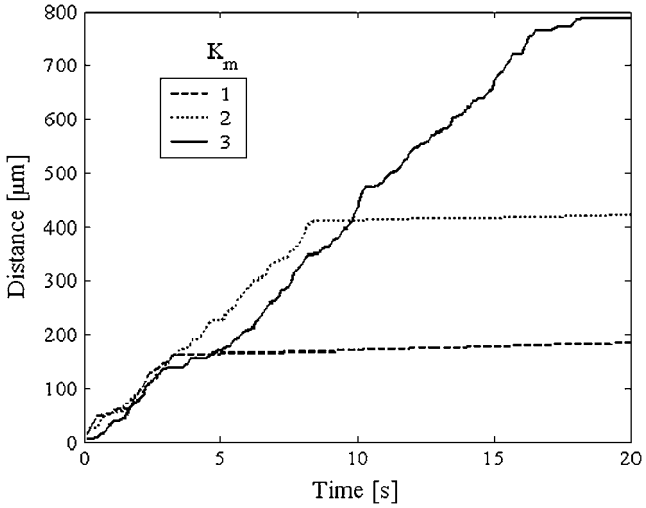

FIGURE 6 Representative simulated rolling trajectories for several values of K_{m}: 1, 3, and 5. Increasing K_{m} prolongs rolling time and distance before arrest. PSGL-1 = 1 molecule/MV; total LFA-1 = 2 molecules/MV; $n_{\text{Hill}} = 3$; $K_{\text{act}} = 0.05$ s.$^{-1}$

PSGL-1 = 1 molecule/MV; total LFA-1 = 2 molecules/MV). As expected, increasing K_m prolongs rolling before arrest. Manipulation of K_m may also produce behavior similar to physiology, for increasing K_m to 10 at these conditions yields a prolonged rolling time of ~86 s (data not shown).

n_{Hill} regulates the dynamics of adhesion depending on K_m

The degree of cooperativity of the activation function is represented by the Hill coefficient, n_{Hill}. Higher values of n_{Hill} correspond to steeper transitions from minimal to maximal response. This parameter reflects the sensitivity of the cell's response to the level of E-selectin expression, which reflects the state of endothelial activation. However, the effect of increased activation sensitivity depends intimately on the value of K_m. Because MAPK shows ultrasensitivity, when S is below K_m, the steepness of the MAPK response with S leads to a very weak activation response and a protracted period of rolling without activation. Hence, when n_{Hill} is large and K_m is large, neutrophils are less easily activated by selectin, a rather surprising result. In contrast, if K_m is small (and n_{Hill} is high), the cell is more likely to be activated as n_{Hill} increases.

The effect of activation function sensitivity in concert with K_m is shown in Fig. 7. We quantify the rolling time, distance before arrest, and activated fraction of integrin at arrest for a cell with 1 PSGL-1 molecule/MV and 2 total integrin molecules/MV, whose $\bar{S}$ in the inactivating state is 1.7. As explained, increasing sensitivity prolongs rolling at high $K_m = 5$ (Fig. 7, *A* and *B*, *circles*). Conversely, increasing n_{Hill} when the K_m (i.e., 0.5) is less than the average selectin bond number results in somewhat earlier arrest than when K_m was high (Fig. 7, *A* and *B*, *diamonds* and *squares*). When K_m is small, increasing n_{Hill} decreases the time to activation. At intermediate K_m values of $1 < K_m < 3$, the rolling time before arrest is nearly independent of n_{Hill}, indicating a regime where only a small amount of selectin is required to activate the pathway. As illustrated in Fig. 7 *C*, the fraction of integrins needed for arrest is not a function of K_m or n_{Hill}, but rather is dictated by the mechanical need to hold the cell stationary.

Effect of shear rate and receptor surface densities

The role of hemodynamic factors in promoting leukocyte activation remains unclear. Does a cell exposed to higher shear rate accrue a larger signal by interacting with a greater length of endothelium and arrest earlier, or does a cell at a smaller shear rate have a more sustained interaction with the endothelium and less velocity to shed before arresting? Intravital microscopy measurements have shown that increases in shear rate promote leukocyte recruitment and rolling flux but that the degree of endothelial activation governs the level of firm adhesion (39). A recent

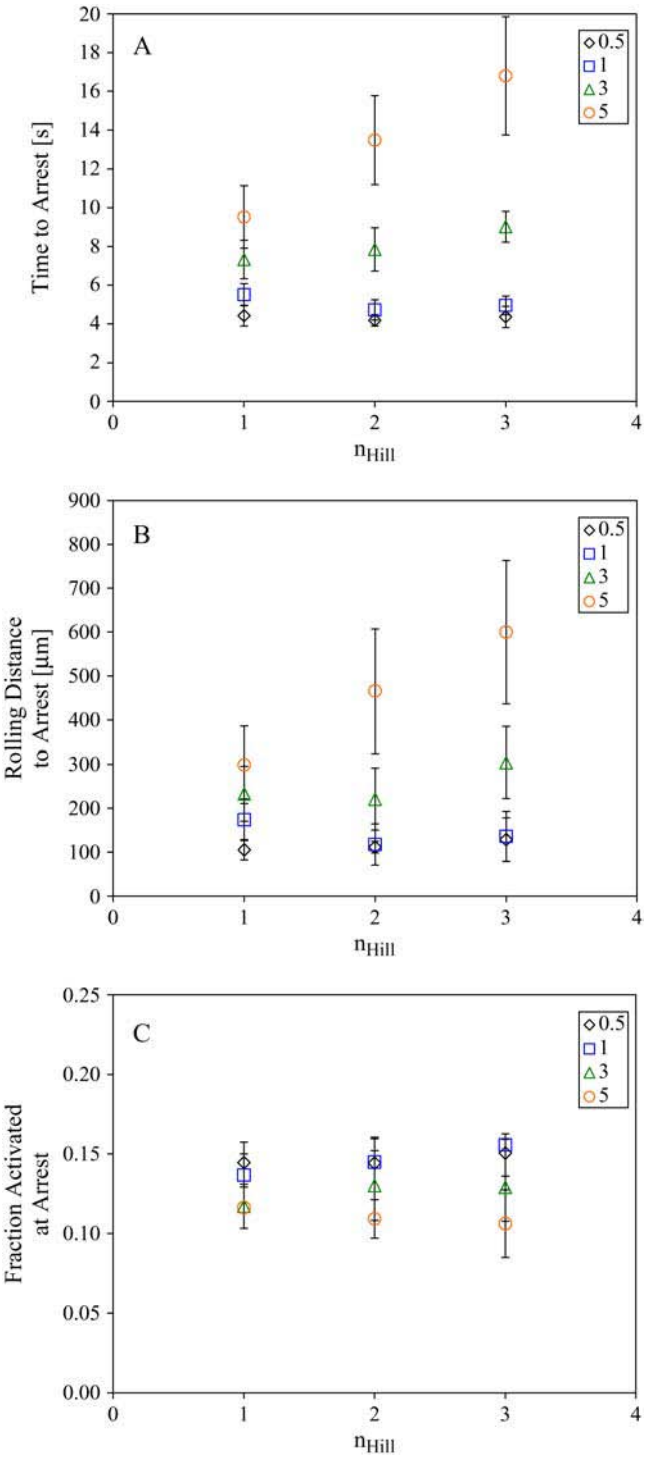

FIGURE 7 The effect of increased cooperativity on arrest depends on K_m. (*A*) Rolling time before arrest as a function of Hill coefficient, n_{Hill}, for four different values of K_m: 0.5 (*diamonds*), 1 (*squares*), 3 (*triangles*), and 5 (*circles*). (*B*) Rolling distance before arrest. (*C*) Fraction of activated LFA-1 at arrest. PSGL-1 = 1 molecule/MV; total LFA-1 = 2 molecules/MV; $K_{act} = 0.05\ s^{-1}$; $N = 8$. Vertical lines indicate standard deviation.

three-dimensional computational model of a deformable leukocyte undergoing selectin-mediated rolling demonstrated that increased shear rate produces a larger cell-substrate contact area that stabilizes rolling, counteracting smaller bond numbers and shorter bond lifetimes under high shear conditions (40).

Before we investigated how increasing the shear rate affects activation and the time to cell arrest, we first needed to choose cell-receptor surface densities that would support both rolling and firm adhesion over a range of shear rates. At higher shear rates of 200 and 300 s^{-1}, the receptor surface density combination used above of 1 molecule PSGL-1/MV and 2 molecules active LFA-1/MV does not support firm adhesion (data not shown). Therefore, no matter how large the value of K_{act}, a system with 1 molecule PSGL-1 /MV and 2 molecules total LFA-1/MV will not transition to arrest at these higher shear rates. However, increasing the receptor surface densities to 4 molecules PSGL-1/MV and 3 molecules total LFA-1/MV restores the ability of the cell to arrest at these higher shear rates. At a shear rate of 200 s^{-1}, this cell with increased surface density rolls when all LFA-1 are resting ($V_{roll} = 20 \pm 4$ μm/s), but it firmly adheres ($V_{roll} < 0.2V_H$) when all LFA-1 are active. The same cell at 300 s^{-1} rolls ($V_{roll} = 192 \pm 13$ μm/s) when all integrins are resting but adheres firmly when all integrins are active ($V_{roll} < 0.2V_H$). For the fully resting cell rolling at 200 s^{-1} shear rate, the average number of PSGL-1 bonds, $\bar{S}_{200}$, is 12.3 $\pm$ 1.8. At 300 s^{-1}, the average PSGL-1 bond number, $\bar{S}_{300}$, is 5.0 $\pm$ 0.5. These average bond numbers are important for choosing activation function parameters, K_m in particular, for appropriate comparisons.

Throughout these shear rate comparisons, we hold constant $K_{act} = 0.01$ s^{-1} and $n_{Hill} = 3$. The value of K_{act} merely sets the timescale of the activation process. The value of n_{Hill} ensures that the activation is ultrasensitive, and the remaining manipulation of K_m permits us to set the level of endothelial activation relative to the cell's state. When $K_m = 10$, $\bar{S}_{200} \approx K_m > \bar{S}_{300}$, the higher shear rate prolongs rolling (Table 3). When $K_m = 5$, $\bar{S}_{200} > K_m \approx \bar{S}_{300}$, and again the higher shear rate prolongs rolling (Table 3). The remaining comparison looks at what happens to a cell at different shear rates, each with an activation function whose K_m is matched to its $\bar{S}$: 1), a shear rate of 200 s^{-1} where $K_m = 10 \approx \bar{S}_{200}$ and 2), a shear rate of 300 s^{-1} where $K_m = 5 \approx \bar{S}_{300}$. Again the cell arrests earlier at the lower shear rate (Table 3).

These results indicate that the potential enhancement in the number of selectin receptor contacts and engagements due to higher shear rates does not increase the input signal to our activation function. The deterministic nature of the activation function holds that the durable ligation of a fixed number of bonds, N, for a given time period, t, will generate the same signal as N bonds that repeatedly form and break X times with a cycle lifetime of t/X. Since the mean number of selectin bonds is lower at higher shear rates, and since activation is proportional to the mean number of selectin bonds at any one time, activation is more pronounced at lower shear rates.

TABLE 3 Rolling time to arrest

	Shear rate (s^{-1})	
K_m	200	300
1	23	74
5	28	>100
10	44	>80

PSGL-1 = 4 molecules/MV; total LFA-1 = 2 molecules/MV; $K_{act} = 0.05$ s^{-1}; and $n_{Hill} = 3$.

DISCUSSION

We successfully created an integrated simulation of neutrophil activation, combining the biophysical model of adhesive dynamics with a simplified model of a MAPK signal transduction pathway. Using experimentally measured selectin and integrin molecular binding parameters in concert with parameters determined from simulation matching to experimental cell-free rolling data, we demonstrated how the gradual change in binding properties of a receptor population can bring about cell deceleration and arrest. By employing modular, manipulable activation, we were able to demonstrate how changing the characteristics of the activation function permit the tuning of the system behavior.

In vivo microscopy of murine cremaster venules following a systemic IL-8 stimulus permitted observation of neutrophil rolling and arrest shear rates on the order of 1000 s^{-1} (38). This work determined mean rolling time before arrest of 86 $\pm$ 16 s, distance rolled before arrest of 270 $\pm$ 58 μm, average rolling velocity of 3.8 $\pm$ 0.4 μm/s, and acceleration of -0.28 ± 0.13 $\mu m/s^2$ for arresting neutrophils. The receptor surface densities and Hill function parameters employed in our simulations were not chosen to best fit this data; rather, the values permit the transition from rolling to arrest to occur over an abbreviated timescale to reduce computational demand. Simulating 100 s of real time, on the order of the transition time observed by Kunkel et al., may require up to 50 h of computational time. By reducing our simulations to one-fifth to one-tenth the physiological timescale, we could more efficiently and reasonably investigate effects of parameters on the system. A simple adjustment in the value of K_{act}, however, allowed us to achieve arrest on the physiological timescale (Fig. 5).

It should be noted that measured cremaster vessel shear rates ($\sim$1000 s^{-1}) are well into the range of shear rates where cell deformation becomes an important factor. Because our rigid cell and microvilli cannot deform, our simulation is not suited to approximate real behavior in this range of shear rates. Although our group recently investigated the role of deformable microvilli on rolling (41), incorporation of this deformation with activation as well as the inclusion of whole-cell deformability remain to be completed.

We have shown here how the parameters $K_{act,}$ K_m, and n_{Hill} affect the dynamics of neutrophil stopping when these parameters describe the activation of β_2-integrins due to occupancy by selectins. In this article, these parameters —$K_{act,}$ K_m, and n_{Hill}—are inputs. However, one might want to know how these parameters might be adjusted in a biological system through alterations in the MAPK pathway. To understand how these parameters can be adjusted systematically, we undertook a systematic exploration of the MAPK pathway, focusing on manipulable system parameters that ultimately lead to changes in $K_{act,}$ $K_{m,}$ and n_{Hill}. The description and results of this exploration are in Appendix A. We found that changing the concentration of MAPKK has a systematic effect on n_{Hill} (Figs. A1 and A2, Appendix 1). Making such a change might be achieved by either transfecting with MAPKK, making a knockout mouse in which MAPK is reduced or increased, or using RNAi to knock down the level of MAPKK. Larger levels of MAPKK lead to higher levels of n_{Hill}. We found that it was not as easy to change $K_{act.}$ For small values of MAPKK, K_{act} could be reduced. A 10-fold decrease in MAPKK leads to a threefold decrease in K_{act}. A 100-fold decrease in MAPKK leads to a 1000-fold decrease in K_{act} (Fig. A3). Alternatively, since K_{act} is a function of the intrinsic activity of the elements of the cascade, a more reasonable way to change K_{act} might be to mutate the enzymes within the cascade to be more or less reactive. Finally, we found that systematic changes in the MAPKK-PPase (MAP kinase kinase-phosphatase) led to systematic changes in K_m, as seen in Figs. A4 and A5. Compared to baseline, there is a monotonic decrease in K_m with a decrease in MAPKK-PPase over four orders of magnitude. This change can be achieved through a MAPKK-PPase knockout or RNAi for partial inhibition. This decrease in K_m leads to an increase in activity, where decreasing K_m makes a fixed level of selectin occupancy more active. Note that the changes we describe in this section are relative changes, compared to baseline, as the levels of these enzymes have not yet been directly measured in neutrophils. Thus, we have identified ways of altering n_{Hill} and K_m and, to a lesser extent, K_{act}, through changes in the concentrations of elements of the MAPK cascade, notably MAPKK and MAPKK-PPase.

Deterministic activation of integrins is the simplest mechanism that can be captured computationally. One can easily imagine more detailed and sophisticated ways of

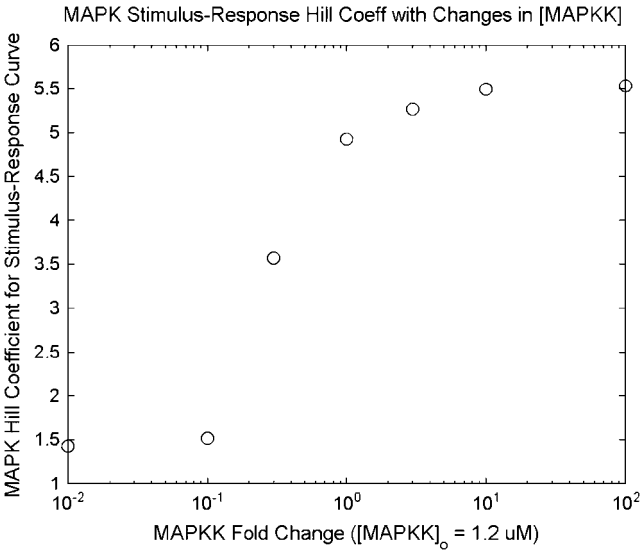

FIGURE A2 Hill coefficients for the MAPK switch over a range of [MAPKK] expressed as fold changes from the initial value (1.2 μM).

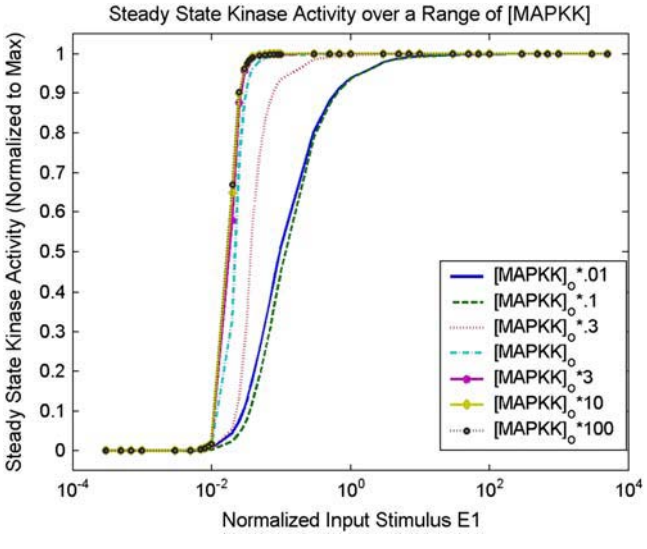

FIGURE A1 MAPK stimulus-response curves based on steady-state kinase activity in response to varying [MAPKK]. Input values are normalized to 1 nM.

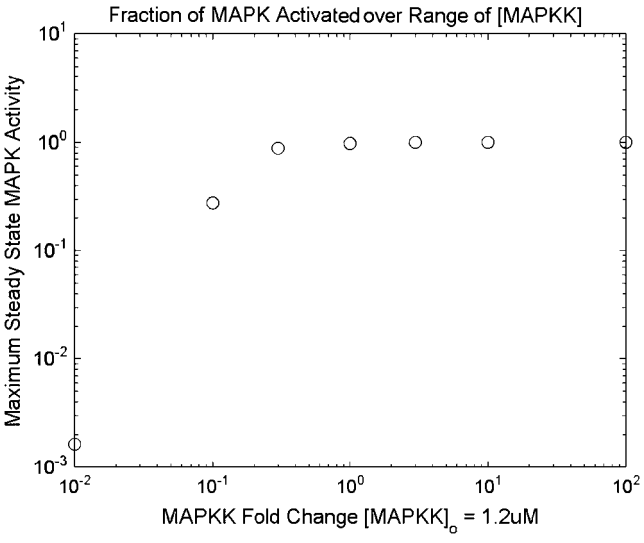

FIGURE A3 Maximum steady-state MAPK activity expressed as a fraction of $[MAPK]_{total}$ in response to varying [MAPKK].

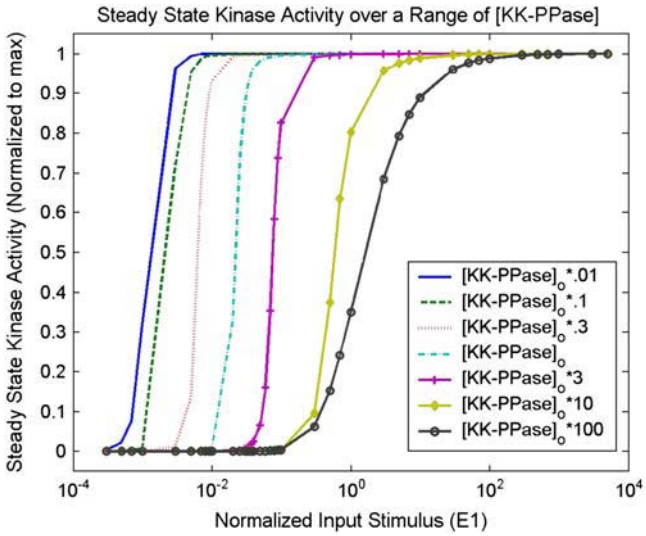

FIGURE A4 MAPK stimulus-response curves based on steady-state kinase activity in response to varying [KK-PPase]. Input values are normalized to 1 nM.

dealing with activation as details emerge. We have neglected the potential importance of spatial relationships in the activation process, such as a GPCR might exhibit. Further, distinct Mac-1 binding and time-dependent Mac-1 surface expression is not considered, but these can be included easily into a deterministic model. However, we find it prudent to refrain from including these phenomena until a fully stochastic model of neutrophil activation is constructed, one that employs a kinetic Monte Carlo algorithm to model signaling pathways (42). We are currently undertaking this project.

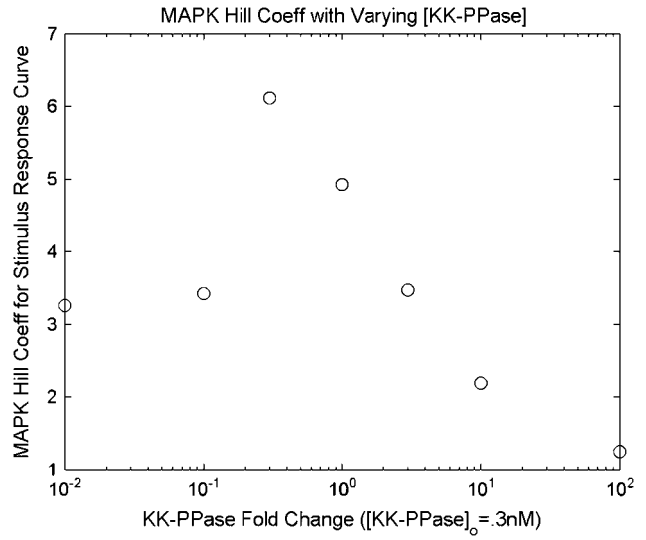

FIGURE A5 EC_{50} values for MAPK stimulus-response curves in response to varying [KK-PPase]. EC_{50} is defined as the concentration of input stimulus corresponding to 50% of the maximal steady-state MAPK activity. EC_{50} values are normalized to 1 nM.

Nevertheless, our calculation illustrates that signaling and mechanics can be integrated in a single model, thus representing a paradigm for how to capture the effects of signaling on cytomechanical phenomena such as adhesion, contraction, and motility. As further details emerge into the exact pathways leading to neutrophil arrest and, perhaps, the added influence of chemokines such as IL-8 or platelet activating factor, our model can be extended to incorporate these effects readily. Our calculations do show, however, that timescales on the order of that seen for activation in vivo can be calculated computationally. Stochastic signal transduction cascades and upregulation of integrin adhesion receptors, such as Mac-1, after cell activation will be added to future generations of this model in our evolution to build the most accurate, integrated model of leukocyte rolling and adhesion possible.

APPENDIX A

In this article, we have embedded a deterministic MAPK signaling cascade within adhesive dynamics to calculate the amount of β_2-integrin activated during leukocyte rolling. The purpose of this appendix is to understand how the activity of the MAPK cascade can be modulated by properties of the MAPK network. Since the MAPK cascade behaves as a switch parameterized by K_{act}, K_m, and the Hill coefficient, n_{Hill}, we sought to understand how features of the network, such as the concentrations of each enzyme within it, modulate these parameters. This then allows us to make testable predictions, where modulations of appropriate enzymes would change K_{act}, K_m, and n_{Hill}, and thus the dynamics of adhesion as we have calculated in this article. Although these parameters are the input to adhesive dynamics simulations, they are the output of the calculations we perform here.

The MAPK cascade is modeled according to the reactions described by Huang and Ferrell (17). The cascade consists of the enzymes MAPKKK, MAPKK, and MAPK, as well as phosphatases that dephosphorylate each species. Table A1 lists each kinase with its activated/phosphorylated forms and phosphatases as well as the baseline concentrations we used for these calculations, as suggested in (17). Note that we do not know the concentrations of these species in neutrophils, as they have not been measured; therefore, the most relevant information we can provide is the relative changes in K_{act}, K_m, and n_{Hill} as the cascade parameters vary, using initial reference concentrations from *Xenopus* used in Huang and Ferrell (17). Each protein species in the cascade is represented by a differential equation describing the reactions in which the protein is involved. Because the ultimate output of the model is steady-state kinase activity, each reaction is modeled with Michaelis-Menten kinetics, as described by Huang and Ferrell (17). Table A2 contains the velocity expression for each reaction included in the cascade. The differential equations are solved using the ode15s solver in MATLAB 6.5.

Protein concentrations and the value of K_m (300 nM) are initially based on those used by Huang and Ferrell (17). The rate constant k_{cat} is assumed to

TABLE A1 Protein specifes in the MAPK cascade

Protein	Active/phosphorylated forms	Initial concentrations
MAPKKK	MAPKKK*	3 nM
MAPKK	MAPKK-P, MAPKK-PP	1.2 μM
MAPK	MAPK-P, MAPK-PP	1.2 μM
KKK-PPase	–	0.3 nM
KK-PPase	–	0.3 nM
K-PPase	–	120 nM

TABLE A2 Velocities based on reactions in MAPK cascade

$V_1 = k_{cat}[E1]_{tot}[KKK]/(K_m + [KKK])$
$V_2 = k_{cat}[KKK\text{-}PPase][KKK^*]/(K_m + [KKK^*])$
$V_3 = k_{cat}[KKK^*][KK]/(K_m + [KK])$
$V_4 = k_{cat}[KK\text{-}PPase][KK\text{-}P]/(K_m + [KK\text{-}P])$
$V_5 = k_{cat}[KKK^*]_{tot}[KK\text{-}P]/(K_m + [KK\text{-}P])$
$V_6 = k_{cat}[KK\text{-}PPase]_{tot}[KK\text{-}PP]/(K_m + [KK\text{-}PP])$
$V_7 = k_{cat}[KK\text{-}PP]_{tot}[K]/(K_m + [K])$
$V_8 = k_{cat}[K\text{-}PPase]_{tot}[K\text{-}P]/(K_m + [K\text{-}P])$
$V_9 = k_{cat}[KK\text{-}PP][K\text{-}P]/(K_m + [K\text{-}P])$
$V_{10} = k_{cat}[K\text{-}PPase][K\text{-}PP]/(K_m + [K\text{-}PP])$

be 10 s^{-1}, which, when used with the K_m and concentrations suggested by Huang and Ferrell (17), successfully reproduce their results (data not shown). MAPK stimulus-response curves are generated by plotting the steady-state levels of MAPK-PP—the active enzyme of the MAPK network. Hill coefficients for the resulting curves are then calculated using the expression $n_{Hill} = \log(81)/\log(EC_{90}/EC_{10})$.

The activity of the MAPK switch is most easily engineered by changing the concentrations of individual kinases and phosphatases. To illustrate, MAPK stimulus-response curves are generated for different concentrations of each kinase and phosphatase. The behavior of MAPK is particularly sensitive to changes in the concentrations of MAPKK and its phosphatase, an observation that was also noted by Huang and Ferrell (17). When the amount of MAPKK in the system is decreased 10-fold from its initial value of 1.2 μM, the Hill coefficient for the MAPK stimulus-response curve falls from 4.9 to 1.4 (Fig. A2), significantly decreasing the ultrasensitivity of the MAPK network. By comparison, a 10-fold decrease in [MAPK] and [MAPKKK] yield n_{Hill}s of 4 and 2.2, respectively (data not shown). As a result, variations in the concentrations of MAPKK and its phosphatase (KK-PPase) are used to illustrate the possibilities for engineering the n_{Hill} value of the MAPK switch.

We varied [MAPKK] 100-fold in each direction and determined how the degree of ultrasensitivity of the resulting stimulus-response curve changes (Figs. A1 and A2). The enzyme activity curves are shown in Fig. A1, and the values of n_{Hill} as a function of relative [MAPKK] in Fig. A2. As [MAPKK] is increased, the MAPK n_{Hill} also increases before reaching a plateau at 5.5 for increases in [MAPKK] 10-fold or greater. The corresponding MAPK curves grow increasingly steeper as [MAPKK] increases (Fig. A1). Physically, the higher values of n_{Hill} suggest that once a threshold level of selectin occupancy is exceeded, the MAPK network will be fully active. Thus, changing n_{Hill} and the steepness of the switch is readily achieved through changing the concentration of MAPKK in cells.

A further consequence of altering [MAPKK] is that for low concentrations of MAPKK, the total level of MAPK activity—or K_{act} in our adhesive dynamics model—is reduced (Fig. A3). For a 10-fold decrease in [MAPKK], K_{act} would be reduced by threefold; for a 100-fold decrease in [MAPKK], K_{act} would decrease 1000-fold. Thus, increases in [MAPKK] modulate the MAPK switch by increasing its sensitivity to input through an increased Hill coefficient, whereas decreases in [MAPKK] affect the MAPK switch by decreasing both K_{act} and n_{Hill}. Since K_{act} encompasses the intrinsic reaction activity of the MAPK network, other changes in it might be achieved through mutation of the enzymes in the cascade, rather than through their amounts.

The phosphatase for MAPKK also regulates the MAPK switch. Although the Hill coefficients do vary somewhat as [KK-PPase] is varied from 100-fold above and below the base concentration (data not shown), the more significant changes are the overall shifts in the stimulus-response curves (i.e., in K_m) for MAPK (Fig. A4). As [KK-PPase] is decreased, the stimulus-response curves shift to lower ranges of input stimulus—lower K_m. This is demonstrated by the decreasing EC_{50} values (K_m) for MAPK stimulus-response with decreasing [KK-PPase] (Fig. A5). As a result, a smaller stimulus will be able to turn the MAPK cascade ''on'' as the [KK-PPase] decreases, corresponding to a requirement that fewer selectin-ligand bonds are required to generate a MAPK ''on'' signal when [KK-PPase] is lowered.

SUPPLEMENTARY MATERIAL

An online supplement to this article can be found by visiting BJ Online at http://www.biophysj.org.

REFERENCES

1. Takagi, J., B. M. Petre, T. Walz, and T. A. Springer. 2002. Global conformational rearrangements in integrin extracellular domains in outside-in and inside-out signaling. *Cell.* 110:599–611.
2. Kim, M., C. V. Carman, and T. A. Springer. 2003. Bidirectional transmembrane signaling by cytoplasmic domain separation in integrins. *Science.* 301:1720–1725.
3. Salas, A., M. Shimaoka, S. Q. Chen, C. V. Carman, and T. Springer. 2002. Transition from rolling to firm adhesion is regulated by the conformation of the I domain of the integrin lymphocyte function-associated antigen-1. *J. Biol. Chem.* 277:50255–50262.
4. Salas, A., M. Shimaoka, A. N. Kogan, C. Harwood, U. H. von Andrian, and T. A. Springer. 2004. Rolling adhesion through an extended conformation of integrin α(L)β(2) and relation to α I and β I-like domain interaction. *Immunity.* 20:393–406.
5. Alon, R., V. Grabovsky, and S. Feigelson. 2003. Chemokine induction of integrin adhesiveness on rolling and arrested leukocytes local signaling events or global stepwise activation? *Microcirculation.* 10: 297–311.
6. Ley, K. 2002. Integration of inflammatory signals by rolling neutrophils. *Immunol. Rev.* 186:8–18.
7. DiVietro, J. A., M. J. Smith, and M. B. Lawrence. 2000. Effect of immobilized IL-8 on neutrophil rolling and adhesion. *FASEB J.* 14:A702.
8. Lum, A. F. H., C. E. Green, G. R. Lee, D. E. Staunton, and S. I. Simon. 2002. Dynamic regulation of LFA-1 activation and neutrophil arrest on intercellular adhesion molecule 1 (ICAM-1) in shear flow. *J. Biol. Chem.* 277:20660–20670.
9. Smith, M. L., T. S. Olson, and K. Ley. 2004. CXCR2- and E-selectin-induced neutrophil arrest during inflammation in vivo. *J. Exp. Med.* 200:935–939.
10. Hidari, K., A. S. Weyrich, G. A. Zimmerman, and R. P. McEver. 1997. Engagement of P-selectin glycoprotein ligand-1 enhances tyrosine phosphorylation and activates mitogen-activated protein kinases in human neutrophils. *J. Biol. Chem.* 272:28750–28756.
11. Evangelista, V., S. Manarini, R. Sideri, S. Rotondo, N. Martelli, A. Piccoli, L. Totani, P. Piccardoni, D. Vestweber, G. de Gaetano, and others. 1999. Platelet/polymorphonuclear leukocyte interaction: P-selectin triggers protein-tyrosine phosphorylation-dependent CD11b/CD18 adhesion: Role of PSGL-1 as a signaling molecule. *Blood.* 93:876–885.
12. Blanks, J. E., T. Moll, R. Eytner, and D. Vestweber. 1998. Stimulation of P-selectin glycoprotein ligand-1 on mouse neutrophils activates β(2)-integrin mediated cell attachment to ICAM-1. *Eur. J. Immunol.* 28:433–443.
13. Smolen, J. E., T. K. Petersen, C. Koch, S. J. O'Keefe, W. A. Hanlon, S. Seo, D. Pearson, M. C. Fossett, and S. I. Simon. 2000. L-selectin signaling of neutrophil adhesion and degranulation involves p38 mitogen-activated protein kinase. *J. Biol. Chem.* 275:15876–15884.
14. Simon, S. I., Y. Hu, D. Vestweber, and C. W. Smith. 2000. Neutrophil tethering on E-selectin activates β(2) integrin binding to ICAM-1 through a mitogen-activated protein kinase signal transduction pathway. *J. Immunol.* 164:4348–4358.
15. Hentzen, E., D. McDonough, L. McIntire, C. W. Smith, H. L. Goldsmith, and S. I. Simon. 2002. Hydrodynamic shear and tethering

through E-selectin signals phosphorylation of p38 MAP kinase and adhesion of human neutrophils. *Ann. Biomed. Eng.* 30:987–1001.

16. Pearson, G., F. Robinson, T. B. Gibson, B. E. Xu, M. Karandikar, K. Berman, and M. H. Cobb. 2001. Mitogen-activated protein (MAP) kinase pathways: regulation and physiological functions. *Endocr. Rev.* 22:153–183.
17. Huang, C. Y. F., and J. E. Ferrell. 1996. Ultrasensitivity in the mitogen-activated protein kinase cascade. *Proc. Natl. Acad. Sci. USA.* 93: 10078–10083.
18. Tandon, R., R. I. Sha'afi, and R. S. Thrall. 2000. Neutrophil β2-integrin upregulation is blocked by a p38 MAP kinase inhibitor. *Biochem. Biophys. Res. Commun.* 270:858–862.
19. Ding, Z. M., J. E. Babensee, S. I. Simon, H. F. Lu, J. L. Perrard, D. C. Bullard, X. Y. Dai, S. K. Bromley, M. L. Dustin, M. L. Entman, C. W. Smith, and C. M. Ballantyne. 1999. Relative contribution of LFA-1 and Mac-1 to neutrophil adhesion and migration. *J. Immunol.* 163:5029–5038.
20. Hentzen, E. R., S. Neelamegham, G. S. Kansas, J. A. Benanti, L. V. McIntire, C. W. Smith, and S. I. Simon. 2000. Sequential binding of CD11a/CD18 and CD11b/CD18 defines neutrophil capture and stable adhesion to intercellular adhesion molecule-1. *Blood.* 95:911–920.
21. Bhatia, S. K., M. R. King, and D. A. Hammer. 2003. The state diagram for cell adhesion mediated by two receptors. *Biophys. J.* 84:2671–2690.
22. Hammer, D. A., and S. M. Apte. 1992. Simulation of cell rolling and adhesion on surfaces in shear-flow: general results and analysis of selectin-mediated neutrophil adhesion. *Biophys. J.* 63:35–57.
23. Chang, K. C., D. F. J. Tees, and D. A. Hammer. 2000. The state diagram for cell adhesion under flow: leukocyte rolling and firm adhesion. *Proc. Natl. Acad. Sci. USA.* 97:11262–11267.
24. Bell, G. I. 1978. Models for specific adhesion of cells to cells. *Science.* 200:618–627.
25. Chang, K. C., and D. A. Hammer. 1999. The forward rate of binding of surface-tethered reactants: effect of relative motion between two surfaces. *Biophys. J.* 76:1280–1292.
26. King, M. R., and D. A. Hammer. 2001. Multiparticle adhesive dynamics. Interactions between stably rolling cells. *Biophys. J.* 81: 799–813.
27. Goldman, A. J., R. G. Cox, and H. Brenner. 1967. Slow viscous motion of a sphere parallel to a plane wall. I. Motion through a quiescent fluid. *Chem. Eng. Sci.* 22:637–651.
28. Goldman, A. J., R. G. Cox, and H. Brenner. 1967. Slow viscous motion of a sphere parallel to a plane wall. II. Couette flow. *Chem. Eng. Sci.* 22:653–659.
29. Shao, J. Y., H. P. Ting-Beall, and R. M. Hochmuth. 1998. Static and dynamic lengths of neutrophil microvilli. *Proc. Natl. Acad. Sci. USA.* 95:6797–6802.
30. Lawrence, M. B., and T. A. Springer. 1991. Leukocytes roll on a selectin at physiological flow-rates: distinction from and prerequisite for adhesion through integrins. *Cell.* 65:859–873.
31. Lei, X., M. R. Lawrence, and C. Dong. 1999. Influence of cell deformation on leukocyte rolling adhesion in shear flow. *J. Biomech. Eng..* 121:636–643.
32. Smith, M. J., E. L. Berg, and M. B. Lawrence. 1999. A direct comparison of selectin-mediated transient, adhesive events using high temporal resolution. *Biophys. J.* 77:3371–3383.
33. Zhang, X. H., E. Wojcikiewicz, and V. T. Moy. 2002. Force spectroscopy of the leukocyte function-associated antigen-1/intercellular adhesion molecule-1 interaction. *Biophys. J.* 83:2270–2279.
34. Chang, K. C., and D. A. Hammer. 2000. Adhesive dynamics simulations of sialyl-Lewis(x)/E-selectin-mediated rolling in a cell-free system. *Biophys. J.* 79:1891–1902.
35. Eniola, A. O., E. F. Krasik, L. A. Smith, G. Song, and D. A. Hammer. 2005. I-domain of lymphocyte function-associated antigen-1 (LFA-1) mediates rolling of polystyrene particles on ICAM-1 under flow. *Biophys. J.* 89:3577–3588.
36. Shimaoka, M., C. F. Lu, R. T. Palframan, U. H. von Andrian, A. McCormack, J. Takagi, and T. A. Springer. 2001. Reversibly locking a protein fold in an active conformation with a disulfide bond: integrin α L I domains with high affinity and antagonist activity in vivo. *Proc. Natl. Acad. Sci. USA.* 98:6009–6014.
37. Shimaoka, M., C. F. Lu, A. Salas, T. Xiao, J. Takagi, and T. A. Springer. 2002. Stabilizing the integrin α M inserted domain in alternative conformations with a range of engineered disulfide bonds. *Proc. Natl. Acad. Sci. USA.* 99:16737–16741.
38. Kunkel, E. J., J. L. Dunne, and K. Ley. 2000. Leukocyte arrest during cytokine-dependent inflammation in vivo. *J. Immunol.* 164:3301–3308.
39. Kim, M. B., and I. H. Sarelius. 2004. Regulation of leukocyte recruitment by local wall shear rate and leukocyte delivery. *Microcirculation.* 11:55–67.
40. Jadhav, S., C. D. Eggleton, and K. Konstantopoulos. 2005. A 3-D computational model predicts that cell deformation affects selectin-mediated leukocyte rolling. *Biophys. J.* 88:96–104.
41. Caputo, K. E., and D. A. Hammer. 2005. Effect of microvillus deformability on leukocyte adhesion explored using adhesive dynamics simulations. *Biophys. J.* 89:187–200.
42. Lee, K. H., A. R. Dinner, C. Tu, G. Campi, S. Raychaudhuri, R. Varma, T. N. Sims, W. R. Burack, H. Wu, O. Kanagawa, M. Markiewicz, P. M. Allen, M. L. Dustin, A. K. Chakraborty, and A. S. Shaw. 2003. The immunological synapse balances T cell receptor signaling and degradation. *Science.* 302:1218–1222.
43. Brunk, D. K., D. J. Goetz, and D. A. Hammer. 1996. Sialyl Lewis(x)/E-selectin-mediate rolling in a cell-free system. *Biophys. J.* 71:2902–2907.
44. Morozov, V. N., and T. Y. Morozova. 1990. What does a protein molecule look like? *Comments Mol. Cell. Biophys.* 6:249–270.
45. Patel, K. D., M. U. Nollert, and R. P. McEver. 1995. P-selectin must extend a sufficient length from the plasma membrane to mediate rolling of neutrophils. *J. Cell Biol.* 131:1893–1902.